Computer-originated planar holographic optical elements

Silviu Reinhorn, Yaakov Amitai, and Albert A. Friesem

We present novel, to our knowledge, methods for the analytical design and recording of planar holographic optical elements in thick materials. The recording of each planar holographic element is done by interference of two aspherical waves that are derived from appropriately designed computer-generated holograms such that the element has the desired grating function for minimizing aberrations and closely fulfills the Bragg condition over its entire area. The design and recording methods are described, along with calculated results of representative elements.

OCIS codes: 090.2890, 090.1760, 090.2900.

1. Introduction

In recent years much effort has been directed toward miniaturization of optical systems to dimensions comparable with those that use electronics.[1–4] One promising approach involves planar optics configurations.[5–8] A general planar configuration comprises a planar transparent substrate that has several holographic optical elements (HOE's) on either one or both sides of the substrate. The holographic elements can function as conventional optical elements such as lenses, beam splitters, polarizers, and mirrors. The light between the HOE's propagates inside the substrate and exploits either total internal reflection or reflective coatings on the substrate surfaces. The alignment of several HOE's that are integrated on one substrate can be done with relatively high accuracy during the fabrication stage. The final planar configuration is rigid, and there is no need for further alignment of the individual HOE's, as is usually necessary with free-space optical configurations.

There are two main approaches to recording HOE's upon planar substrates. One involves direct recording and lithographic techniques, and the other, holographic interferometric recording. With direct recording and lithographic techniques a computer-generated mask is transferred to form elements as surface-relief gratings that can perform almost any arbitrary wave-front transformations. Unfortunately, for planar configurations the required grating period of the relief grating is quite small. For example, grating period Λ, which couples a normally incident wave into a transparent substrate so that the diffracted beam will be trapped inside the substrate by total internal reflection, is $\Lambda = \lambda/(n \sin \theta)$, where λ is the wavelength of the incident wave, n is the index of refraction of the substrate, and θ is the diffraction angle inside the substrate. When θ is equal to the critical angle of the substrate, then $\Lambda = \lambda$, which leads to a grating with line widths of the order of $\lambda/2$. As a result, for visible radiation only gratings that have binary profiles can be recorded by currently available methods for electron-beam direct writing. Such gratings have a relatively low diffraction efficiency, typically below 50%.

One way to improve the diffraction efficiency is to design planar elements with a moderate off-axis angle inside the substrate (10°) so the needed gratings have periods of the order of 4λ. Such gratings can be recorded with multilevel lithography to yield blazed profiles, thereby improving the diffraction efficiency significantly (more than 90% for eight levels) over a relatively wide range of incident angles. When such planar elements are used the substrate surfaces must be coated with reflective materials to trap the light inside the substrate. Unfortunately, the reflective materials are lossy, so after the many internal reflections the overall light efficiency is again relatively low.

For planar optical configurations in which the elements are recorded as surface-profile gratings we must impose certain geometrical conditions to ensure

The authors are with the Department of Physics of Complex Systems, Weizmann Institute of Science, Rehovot 76100, Israel.

Received 20 August 1997; revised manuscript received 6 January 1998.

0003-6935/98/143031-07$15.00/0

that undesirable interaction between internally reflected rays and the planar elements does not occur. Specifically, we must choose the proper dimensions and locations for the planar HOE's as well as the proper thicknesses for the substrates. The light rays that are diffracted by the planar element into the substrate must propagate a lateral distance that is greater than the aperture D of the element to avoid undesired outward diffraction from the same element. The ratio between the aperture size of the planar element and the substrate thickness T is thus limited by $D/T \leq 2 \tan \theta$, where θ is greater than the critical angle.

With holographic recording it is possible to record volume phase gratings of high spatial frequencies, so the incident beam will be diffracted into the substrate with high diffraction efficiency at an internal angle larger than the critical angle. Here there is no need for any reflective coatings, so the substrate remains transparent and there is little, if any, reflection loss. Moreover, a planar holographic lens in volume phase materials has a variable grating period, in which the local Bragg condition varies along the area of the grating. In such a case, unlike for surface-relief gratings, the internally propagating light rays will diffract outward from the substrate only at desired locations where they satisfy the local Bragg conditions.[9]

For ensuring that geometric and chromatic aberrations are minimized and the diffraction efficiencies are maximized, several optimization design methods for the grating function of HOE's were developed, both for low diffraction angles[10] as well as for HOE's with high diffraction angles.[11] In all these methods it is usually necessary to resort to aspherical wave fronts to record the desired grating functions. Such wave fronts can be derived from interim holograms designed in accordance with a recursive design technique[12] as well as from computer-generated holograms (CGH's).[13]

With the recursive technique the final element is recorded with predistorted aspherical waves that originate from interim holograms that were recorded and read out with either spherical or even predistorted aspherical waves. The technique can be extended to include predistorted waves that will maximize the diffraction efficiency as well.[14] Yet for practical considerations the number of iterations must be limited, so the recursive design technique is usually confined to elements with relatively simple grating functions.

When the aspherical wave fronts for recording a HOE are derived from CGH's,[15] it is possible to obtain more-general grating functions for which the geometric and chromatic aberrations are minimized. The diffraction efficiency for such a computer-originated holographic optical element, however, is typically rather low. Some attempts to increase the diffraction efficiency were reported for relatively simple and specific elements.[14]

In this paper we present a new design method and simple configuration for recording generalized computer-generated holographic optical elements that have both minimum aberrations and maximum diffraction efficiencies. The design method exploits a design in which the grating vector of the HOE is optimized and a recording configuration in which the CGH's are both on the same substrate. It leads to a final HOE that has the small grating periods needed for planar configurations and arbitrary three-dimensional grating functions. Such characteristics are difficult, if not impossible, to obtain with the earlier design methods.

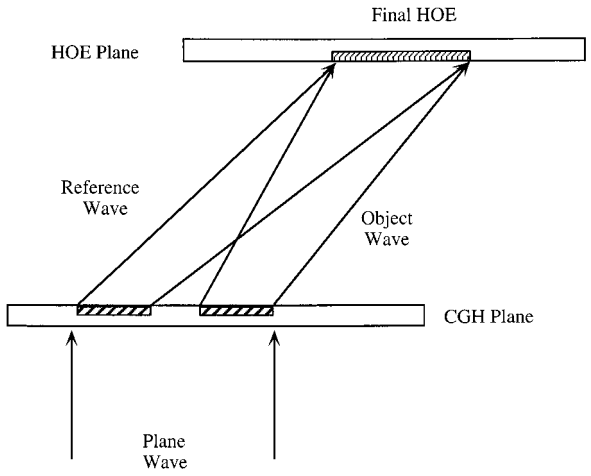

Fig. 1. Geometry for recording the final HOE with recording wave fronts derived from CGH's.

2. Design Considerations

The recording configuration of our device, in which the aspherical wave fronts are derived from two CGH's that are on one substrate, is shown in Fig. 1. When both CGH's are formed on the same substrate it is possible to control the distance between them with great accuracy. This substrate can be aligned parallel to the final HOE plane so the wave fronts impinging upon the holographic recording medium can be controlled accurately. For planar optical elements it is usually required that one of the recording beams impinge upon the holographic recording medium at a large off-axis angle. For example, if the required off-axis angle of the reference beam is 60° and the recording wavelength is 0.5 μm, the grating period of the CGH is $\Lambda = 0.5/(\sin 60) = 0.577$ μm. Consequently, the CGH's must be recorded with electron-beam direct writing. With today's available technology it is possible to record only binary gratings with such fringe density. Fortunately, the diffraction efficiencies of the CGH's do not influence the diffraction efficiency of the final element, so the CGH's can be recorded as binary gratings, usually a much simpler procedure.

When one is dealing with HOE's it is mainly the phases of the recording waves that establish the relevant diffraction relations, given by

$$\phi_i(x, y) = \phi_c(x, y) \pm \phi_h(x, y), \tag{1}$$

where ϕ_i and ϕ_c denote the phases of the diffracted image and reconstructing waves, respectively, the plus or minus sign refers to the positive and negative first diffraction orders from the hologram, and ϕ_h denotes the holographic grating function, given by

$$\phi_h(x, y) = \phi_o(x, y) - \phi_r(x, y), \tag{2}$$

where ϕ_o and ϕ_r denote the phases of the object and the reference recording waves, respectively. Equation (1) is the basic holographic equation, indicating that a HOE acts as a wave-front transforming element, i.e., it transforms the incoming wave front ϕ_c into the output wave front ϕ_i. Usually, when there is a range of possible input and output wave fronts the grating function $\phi_h(x, y)$ must perform the desired transformation with minimum aberrations[16–18] by exploitation of some optimization method.[12,19,20] Such methods can exploit the fact that $\phi_h(x, y)$ can be an arbitrary two-dimensional function, so there is an infinite set of two-dimensional functions $\phi_o(x, y)$ and $\phi_r(x, y)$ that can generate it.

It is often more convenient to deal with light rays instead of wave fronts, especially when one is calculating the diffraction efficiency from volume gratings by the coupled-wave theory. The normalized propagating vectors, which can be regarded as the direction cosines of the rays, can be written as

$$\hat{k}_q = \frac{\lambda_p}{2\pi} \nabla \phi_q, \tag{3}$$

where $\mathbf{q} = o, r, c, i$ and $p = o, c$, ∇ is the gradient operator with respect to the spatial coordinates x and y, λ_o denotes the recording wavelength, and λ_c denotes the reconstructing wavelength. Equation (3) represents a two-dimensional projection of the propagation vector upon a plane perpendicular to the direction of propagation. The grating vector of the hologram is defined as

$$\mathbf{k}_h = \frac{\lambda_o}{2\pi} \nabla \phi_h(x, y) = \frac{\lambda_o}{\Lambda_x(x, y)} \hat{x} + \frac{\lambda_o}{\Lambda_y(x, y)} \hat{y}, \tag{4}$$

where $\Lambda_x(x, y)$ and $\Lambda_y(x, y)$ are the grating spacings in the x and the y directions, respectively.

When the HOE is recorded in thick materials, $\mathbf{k}_h$ has a three-dimensional grating vector distribution. The lateral two-dimensional distribution influences the optical wave-front transformation properties of the HOE, whereas the third dimension z is related to the mechanism of transferring energy from the incident wave to the diffracted wave. The grating spacings $\Lambda_x(x, y)$ and $\Lambda_y(x, y)$ in the x and the y directions have the forms

$$\Lambda_x(x, y) = \frac{\lambda_o}{\sin \beta_o(x, y) \cos \alpha_o(x, y) - \sin \beta_r(x, y) \cos \alpha_r(x, y)},$$

$$\Lambda_y(x, y) = \frac{\lambda_o}{\sin \alpha_o(x, y) - \sin \alpha_r(x, y)}, \tag{5}$$

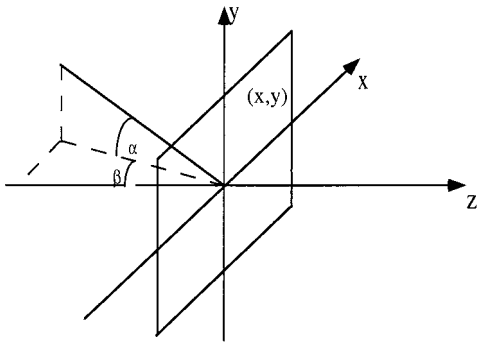

Fig. 2. Coordinate system for recording and readout of the HOE.

where β_o and β_r are the angles between the projection of the propagating vectors of the object and reference waves, respectively, on meridional plane (x, z) and the z axis, and α_o and α_r are the angles between the actual propagation vectors and the meridional plane, respectively, as illustrated in Fig. 2. The diffraction relations can now be written as

$$\begin{aligned} k_{x_i} &= k_{x_c} \pm \mu k_{x_h}, \\ k_{y_i} &= k_{y_c} \pm \mu k_{y_h}, \\ k_{z_i} &= \pm(1 - k_{x_i}^2 - k_{y_i}^2)^{1/2}, \end{aligned} \tag{6}$$

where $\mu = \lambda_c/\lambda_o$. The sign of k_z is determined in accordance with

$$\begin{aligned} &\text{sign}(k_{z_i}) = \text{sign}(k_{z_c}), && \text{(transmission hologram)}, \\ &\text{sign}(k_{z_i}) = -\text{sign}(k_{z_c}), && \text{(reflection hologram)}. \end{aligned}$$

To obtain a high diffraction efficiency it is necessary to satisfy the Bragg condition over the entire area of the HOE. This is achieved when the three-dimensional grating vector $\mathbf{k}_h$ fulfills the condition

$$\mathbf{k}_h(x, y) = \hat{k}_i(x, y) - \hat{k}_c(x, y) = \frac{1}{\mu} [\hat{k}_o(x, y) - \hat{k}_r(x, y)]. \tag{7}$$

In general, it is difficult to record a HOE that simultaneously has low aberrations and high diffraction efficiency over its entire area. Specifically, the aberrations and the image geometry depend on the two-dimensional grating distribution across the surface of the holographic element,[16–18] whereas the diffraction efficiency is determined by the three-dimensional grating distribution.[9] In other words, it is difficult to fulfill the condition set forth in Eq. (7), i.e., to obtain a set of conserving vectors from which we can find realizable phases for the recording waves, ϕ_o and ϕ_r. There are two situations when Eq. (7) can be easily satisfied: first, when $\mu = 1$, i.e., there is no wavelength difference between recording and readout, and second, when $\mathbf{k}_h$ is a one-dimensional function, i.e., $\mathbf{k}_h(x)$.

In planar optical elements with the usual high off-axis angle there is one direction in the hologram plane where the grating spacing is much smaller than that in the orthogonal direction. Typically, the

off-axis angle is aligned with respect to the x axis, so $\Lambda_x < \Lambda_y$, for example, in planar elements in which the light is trapped inside the substrate by total internal reflection, where θ is approximately 45°, according to Eq. (5), $\Lambda_x/\Lambda_y < 0.025$. In such elements the angular and wavelength selectivities because of the Bragg condition are greater in the x direction than in the y direction.[9] Thus we can exploit the advantage that $\mathbf{k}_h$ is almost a one-dimensional function. Accordingly, we develop a design procedure, assuming that the recording setup is that illustrated in Fig. 1. Our design method is appropriate for a situation in which the final desired HOE is recorded as a volume grating that can have a two-dimensional grating function. In addition, its readout wavelength might be different from that of the recording. Our design procedure has two stages. First, we calculate the phases of the object and the reference waves at the HOE plane that form the desired grating function, which simultaneously nearly fulfills the Bragg condition over an area as large as possible. Second, we trace these wave fronts to the CGH's plane by an ordinary ray-tracing approach.[21]

To calculate the needed object and reference waves we begin with the desired grating function $\phi_{h_d}(x, y)$ of the HOE and determine the desired grating vector $\mathbf{k}_{h_d}(x, y)$ according to

$$\mathbf{k}_{h_d}(x, y) = \frac{\lambda_c}{2\pi} \nabla \phi_{h_d}(x, y). \tag{8}$$

The components of the desired grating vector that fulfill the relations for the first (+1) diffraction order are

$$\begin{aligned} k_{x_{h_d}}(x, y) &= k_{x_i}(x, y) - k_{x_c}(x, y), \\ k_{y_{h_d}}(x, y) &= k_{y_i}(x, y) - k_{y_c}(x, y), \\ k_{z_{h_d}}(x, y) &= [1 - k_{x_{h_d}}{}^2(x, y) - k_{x_{h_d}}{}^2(x, y)]^{1/2}. \end{aligned} \tag{9}$$

Equation (7) can be solved to yield $\hat{k}_o$ and $\hat{k}_r$ in the presence of a wavelength shift when the grating vector of the HOE is one dimensional. To obtain such a one-dimensional vector we set $\mathbf{k}_q(x, y) = \mathbf{k}_q(x, y = 0)$, where $q = i, c, o, r$. Now we let $\mathbf{k}_r(x, y)$ be

$$\mathbf{k}_r(x, y) = \mathbf{k}_r(x, y = 0). \tag{10}$$

Because $\mathbf{k}_r(x, y)$ depends on only the x coordinate it is a conserving vector, so we can obtain a unique solution for $\phi_{r_d}(x, y)$ by using

$$\phi_{r_d}(x, y) = \frac{2\pi}{\lambda_o} \int \mathbf{k}_r(x, y) \mathbf{d}x. \tag{11}$$

Here the integration constant was set arbitrarily to 0. Then, in accordance with Eq. (2), we calculate the desired phase of the object wave $\phi_{o_d}(x, y)$ as

$$\phi_{o_d}(x, y) = \phi_{h_d}(x, y) + \phi_{r_d}(x, y). \tag{12}$$

When the object and reference waves that have the phases given in Eqs. (11) and (12) interfere, the desired grating distribution is obtained, and the Bragg condition is completely fulfilled along the line $y = 0$. The deviation from the Bragg condition over the rest of the area is quite small because of the reasons mentioned above. Finally, these calculated wave fronts are transferred to the CGH plane by one of the wave-front transference methods.[21]

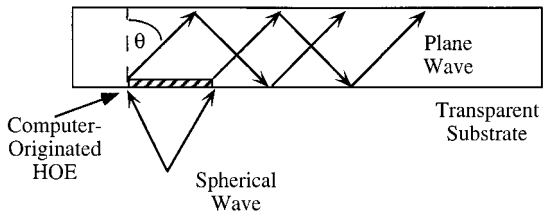

Fig. 3. Computer-originated holographic optical element in a planar configuration.

3. Calculated Results

To verify our design we calculated the diffraction efficiencies of several planar HOE's that were recorded with waves from CGH's, i.e., computer-originated HOE's. These calculations exploited the analytical coupled-wave theory.[9] Initially we considered a planar holographic lens that operates in the geometry depicted in Fig. 3. This lens transforms an on-axis spherical wave that originated from a point source located at coordinates (0, 0, z) into an off-axis plane wave that is trapped inside the substrate by total internal reflection. The grating function $\phi_{h_d}{}^{\text{spherical}}$ of the lens has the form

$$\phi_{h_d}{}^{\text{spherical}}(x, y) = -\frac{2\pi}{\lambda_c}[(x^2 + y^2 + z^2)^{1/2} - nx \sin \theta], \tag{13}$$

where z is the focal distance, n is the substrate's index of refraction, and θ is the off-axis angle inside the substrate.

To illustrate our design procedure we chose the specific example of the spherical grating function given in Eq. (13). To record such a grating function we must solve Eq. (7) explicitly to find ϕ_{r_d} and ϕ_{o_d}. We begin with a reconstruction spherical wave whose normalized propagation vectors inside the substrate are

$$\begin{aligned} k_{x_c} &= -\frac{x}{n(x^2 + y^2 + z^2)^{1/2}}, \\ k_{y_c} &= -\frac{y}{n(x^2 + y^2 + z^2)^{1/2}}, \\ k_{z_c} &= (1 - k_{x_c}{}^2 - k_{y_c}{}^2)^{1/2}. \end{aligned} \tag{14}$$

The normalized propagation vectors of the desired diffracted beam inside the substrate are

$$\begin{aligned} k_{x_i} &= \sin \theta, \\ k_{y_i} &= 0, \\ k_{z_i} &= (1 - k_{x_i}{}^2 - k_{y_i}{}^2)^{1/2}. \end{aligned} \tag{15}$$

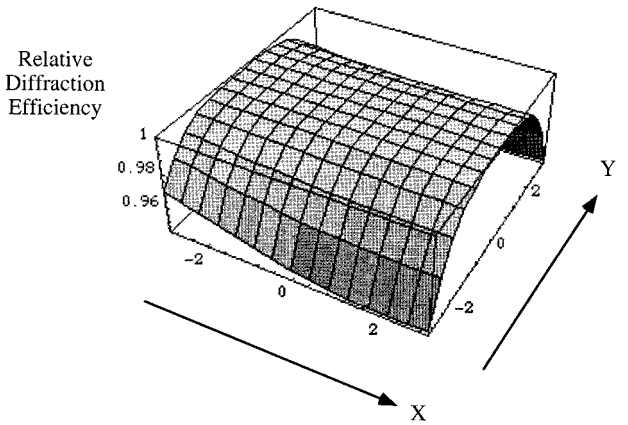

Fig. 4. Calculated diffraction efficiency for a spherical lens that has a grating function $\phi_{h_d}^{\text{spherical}}$.

Now we insert Eqs. (14) and (15) into Eq. (7) and let $k_{y_c} = k_{y_i} = 0$ to calculate $\mathbf{k}_o(x, y = 0)$ and $\mathbf{k}_r(x, y = 0)$. For convenience, let us define

$$S \equiv -\mu(k_{x_i} - k_{x_c}),$$
$$C \equiv -\mu(k_{z_i} - k_{z_c}). \tag{16}$$

Thus Eq. (7) simplifies to a set of two equations with four coupled variables, given by

$$k_{x_o} - k_{x_r} = S,$$
$$k_{z_o} - k_{z_r} = C. \tag{17}$$

Using the relations $k_{z_o} = \sqrt{1 - k_{x_o}}$ and $k_{z_r} = \sqrt{1 - k_{x_r}}$ and performing some mathematical manipulations yield

$$k_{x_r} = \frac{-b + \sqrt{b^2 - 4ac}}{2a}, \tag{18}$$

where

$$a = 4S^2 + 4C^2,$$
$$b = 4S^3 + 4C^2S,$$
$$c = S^4 + C^4 - 4C^2 + 2C^2S^2.$$

By inserting the result obtained in Eq. (18) into Eq. (11) we can find the phase of the reference recording beam Φ_{r_d}, and then by using Eq. (12) we find the phase of the object recording beam Φ_{o_d}.

We now design a CGH such that the holographic lens will be recorded with $\lambda_o = 514.5$ nm and reconstructed with $\lambda_c = 800$ nm, the substrate index of refraction is $n = 1.5$, and the off-axis angle is $\theta = 45°$. We calculate the diffraction efficiency as a function of the coordinates x and y, as illustrated in Fig. 4. In the calculation we assume that the emulsion thickness of the recording material is 10 μm and that the focal distance z of the lens is 10 mm. The results indicate that the relative diffraction efficiency is 100% along the line $y = 0$, as expected, and it drops to approximately 95% at the edges. These results are calculated for an aperture for which the lens has an f-number of 1.66, which is quite small.

Then we compare the results from two representative planar holographic cylindrical lenses. The first has a grating function $\phi_{h_d}^{\text{cylindrical},x}$ of the form

$$\phi_{h_d}^{\text{cylindrical},x}(x, y) = -\frac{2\pi}{\lambda_c}(\sqrt{x^2 + z^2} - nx \sin\theta). \tag{19}$$

The second lens has a grating function $\phi_{h_d}^{\text{cylindrical},y}$ of the form

$$\phi_{h_d}^{\text{cylindrical},y}(x, y) = -\frac{2\pi}{\lambda_c}(\sqrt{y^2 + z^2} - nx \sin\theta). \tag{20}$$

The first cylindrical lens transforms an on-axis cylindrical wave, emerging from a line source parallel to the y axis along the line $(0, y, z = 10)$, into an off-axis plane wave that is coupled inside the substrate by means of total internal reflection. The second cylindrical lens transforms an on-axis cylindrical wave, emerging from a line source parallel to the x axis along the line $(x, 0, z = 10)$, into an off-axis plane wave.

The diffraction efficiencies of the cylindrical lenses are calculated with the same parameters that were

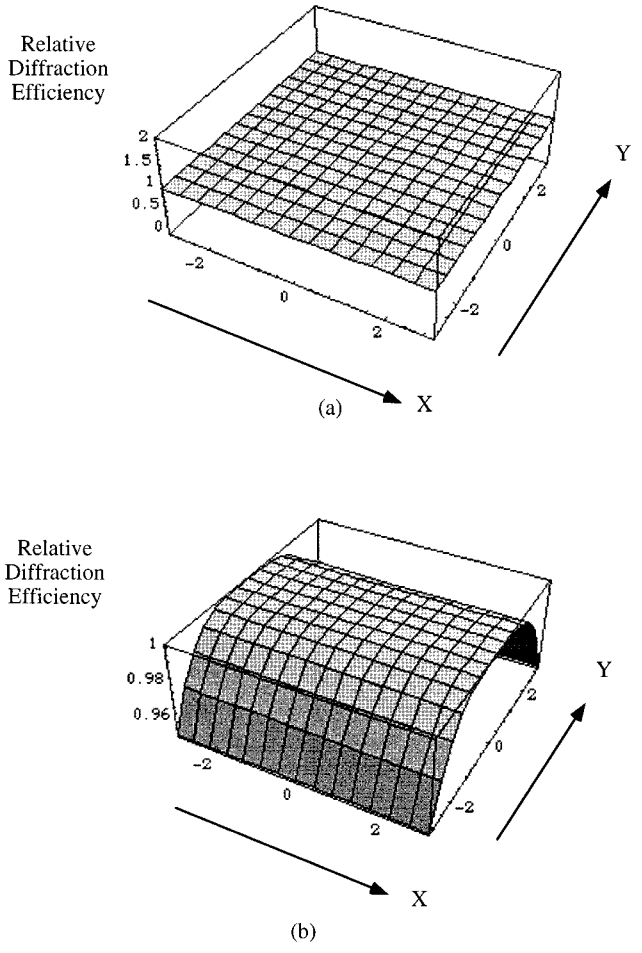

Fig. 5. Calculated diffraction efficiency for cylindrical lenses that have grating functions (a) $\phi_{h_d}^{\text{cylindrical},x}$ and (b) $\phi_{h_d}^{\text{cylindrical},y}$.

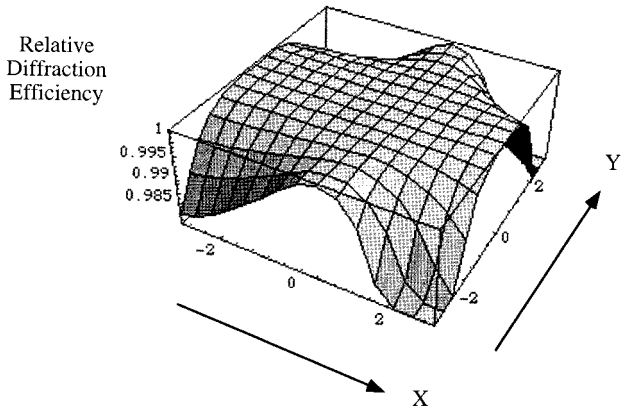

Fig. 6. Calculated diffraction efficiency for an imaging lens with a grating function $\phi_{h_d}^{\text{imaging}}$.

used for the spherical lens above. The results of these calculations are presented in Fig. 5. For the grating function $\phi_{h_d}^{\text{cylindrical},x}$, where all the optical power is in the x direction, the relative diffraction efficiency is 100% over the entire area of the lens, as shown in Fig. 5(a). On the other hand, for the grating function $\phi_{h_d}^{\text{cylindrical},y}$, where the optical power is only in the y direction, the relative diffraction efficiency is 100% along only the $y = 0$ line, and it drops symmetrically with respect to the y axis to approximately 95% at the edges, as can be seen from Fig. 5(b). This is so because the design method requires that the final grating fulfill exactly the Bragg condition on the $y = 0$ line. Thus, for the first cylindrical lens whose grating function and grating vector do not depend on the y coordinate, the Bragg condition is fulfilled over the entire area, whereas for the second lens whose grating function and grating vector depend on x and y coordinates, the deviation from the Bragg condition increases as a function of the distance from the y axis.

Now we consider a planar holographic imaging lens whose grating function has the form

$$\phi_{h_d}^{\text{imaging}}(x, y) = -\frac{2\pi}{\lambda_c}\{(x^2 + y^2 + z^2)^{1/2} - n[(x - x_o)^2 + y^2 + z_o^2]^{1/2}\}. \quad (21)$$

This lens transforms an on-axis spherical wave emerging from a point source located at coordinates $(0, 0, z)$ into a spherical wave that converges to a point inside the substrate at coordinates $(x_o, 0, z_o)$. For the calculations we use $x_o = z_o = 10$ mm, so the off-axis angle of the central diffracted ray is also 45°. The calculated results of the relative diffraction efficiency as a function of the lens aperture are shown in Fig. 6. As is evident, the relative diffraction efficiency along the $y = 0$ line is 100%, and at the edges it drops to 98.5%.

4. Concluding Remarks

We have presented a novel method for designing computer-originated HOE's that can be recorded with a wavelength that is different from that used for readout and still obtain exactly the desired grating function that closely fulfills the Bragg condition over the entire area of the HOE. This method is especially appropriate for recording HOE's that must operate at a wavelength for which there are no suitable recording materials. Also, it is appropriate for planar HOE's whose spatial frequencies are high and must be recorded with a wavelength that it is shorter than that of readout.

The CGH's from which the recording waves for the final HOE's are derived are fabricated with the aid of electron-beam direct writing and advanced lithographic technology. The CGH for the reference wave is fabricated as a one-dimensional grating, i.e., it contains only straight lines that have high spatial frequencies. The CGH for the object wave front is fabricated as a grating with curved lines and relatively low spatial frequencies. Thus one can fabricate CGH's with relative ease by exploiting current electron-beam and lithographic technologies.

This project was supported in part by the Israeli Ministry of Science and Technology.

References

1. R. T. Chen, H. Lu D. Robinson, M. Wang, G. Savant, and T. Jannson, "Guided wave planar optical interconnects using highly multiplexed polymer waveguide holograms," J. Lightwave Technol. **10,** 888–897 (1992).
2. H. M. Ozaktas, Y. Amitai, and J. W. Goodman, "Comparison of system size for some optical interconnection architectures and the folded multi-facet architecture," Opt. Commun. **82,** 225–228 (1991).
3. A. N. Putilin, V. N. Morozov, Q. Huang, and J. H. Caufield, "Waveguide holograms with white light illumination," Opt. Eng. **30,** 1615–1619 (1991).
4. I. Glaser, "Compact lenslet array based holographic correlator/convolver," Opt. Lett. **20,** 1565–1567 (1995).
5. J. Jahns and S. Walker, "Imaging with planar optical systems," Opt. Commun. **76,** 313–317 (1989).
6. R. K. Kostuk, Y. T. Huang, D. Hetherington, and M. Kato, "Reducing alignment and chromatic sensitivity of holographic optical interconnects with substrate-mode holograms," Appl. Opt. **28,** 4939–4944 (1989).
7. Y. Amitai, "Design of wavelength-division multiplexing/demultiplexing using substrate mode holographic elements," Opt. Commun. **98,** 24–28 (1993).
8. S. Reinhorn, S. Gorodeisky, A. A. Friesem, and Y. Amitai, "Fourier transformation with planar holographic doublet," Opt. Lett. **20,** 495–497 (1995).
9. H. Kogelnik, "Coupled wave theory for thick holograms and their applications," Bell. Syst. Tech. J. **48,** 2909–2947 (1969).
10. K. Winick, "Designing efficient aberration-free holographic lenses in the presence of a construction-reconstruction wavelength shift," J. Opt. Soc. Am. **72,** 143–148 (1982).
11. Y. Amitai and J. Goodman, "Design of substrate-mode holographic interconnects with different recording and readout wavelengths," Appl. Opt. **30,** 2376–2381 (1991).
12. Y. Amitai and A. A. Friesem, "Design of holographic optical elements by using recursive techniques," J. Opt. Soc. Am. **5,** 702–712 (1988).
13. W. H. Lee, "Binary synthetic holograms," Appl. Opt. **13,** 1677–1682 (1974).
14. Y. Amitai and A. A. Friesem, "Combining low aberration and

high diffraction efficiency in holographic optical elements," Opt. Lett. **13,** 883–885 (1988).
15. R. C. Fairchild and J. R. Fienup, "Computer originated hologram lenses," Opt. Eng. **21,** 133–140 (1982).
16. J. N. Latta, "Computer-based analysis of holography using ray tracing," Appl. Opt. **10,** 2698–2710 (1971).
17. R. W. Meier, "Magnification and third-order aberrations in holography," J. Opt. Soc. Am. **55,** 987–992 (1965).
18. E. B. Champagne, "Nonparaxial imaging magnification and aberration properties in holography," J. Opt. Soc. Am. **57,** 51–55 (1967).
19. E. Hasman and A. A. Friesem, "Analytic optimization for holographic optical elements," J. Opt. Soc. Am. A **6,** 62–72 (1989).
20. J. Kedmi and A. A. Friesem, "Optimized holographic optical element," J. Opt. Soc. Am. A **3,** 2011–2018 (1986).
21. E. Socol, Y. Amitai, and A. A. Friesem, "Design of planar optical interconnects," in *Ninth Meeting on Optical Engineering in Israel*, I. Shladov, ed., Proc. SPIE **2426,** 433–442 (1995).